

Asynchronous Large Language Model Enhanced Planner for Autonomous Driving

Yuan Chen^{1,2*}, Zi-han Ding^{1*}, Ziqin Wang^{1*}, Yan Wang^{2†}, Lijun Zhang¹, and Si Liu^{1†}

¹ Beihang University

² AIR, Tsinghua University

{chenyuan1, wzqin, ljzhang, liusi}@buaa.edu.cn

zihanding819@gmail.com

wangyan@air.tsinghua.edu.cn

Abstract. Despite real-time planners exhibiting remarkable performance in autonomous driving, the growing exploration of Large Language Models (LLMs) has opened avenues for enhancing the interpretability and controllability of motion planning. Nevertheless, LLM-based planners continue to encounter significant challenges, including elevated resource consumption and extended inference times, which pose substantial obstacles to practical deployment. In light of these challenges, we introduce *AsyncDriver*, a new asynchronous LLM-enhanced closed-loop framework designed to leverage scene-associated instruction features produced by LLM to guide real-time planners in making precise and controllable trajectory predictions. On one hand, our method highlights the prowess of LLMs in comprehending and reasoning with vectorized scene data and a series of routing instructions, demonstrating its effective assistance to real-time planners. On the other hand, the proposed framework decouples the inference processes of the LLM and real-time planners. By capitalizing on the asynchronous nature of their inference frequencies, our approach has successfully reduced the computational cost introduced by LLM, while maintaining comparable performance. Experiments show that our approach achieves superior closed-loop evaluation performance on nuPlan’s challenging scenarios. The code and dataset are available at <https://github.com/memberRE/AsyncDriver>.

Keywords: Autonomous Driving · Large Language Models · Motion Planning

1 Introduction

Motion planning plays a pivotal role in autonomous driving, garnering significant interest due to its direct impact on vehicle navigation and safety. One particularly noteworthy evaluation approach is the employment of closed-loop simulation, which involves the dynamic development of driving scenarios that

* Equal contribution. † Corresponding author.

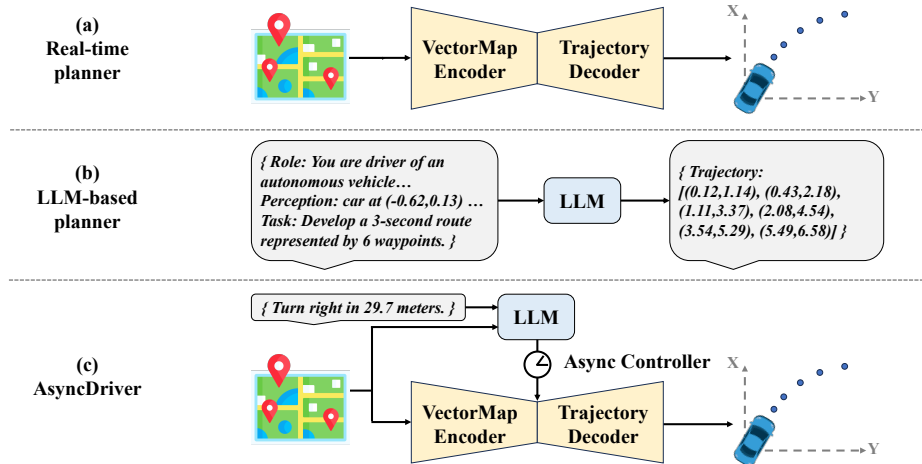


Fig. 1: Comparative Overview of Learning-based Autonomous Driving Planning Frameworks. (a) Real-time planner: Offers quick inference but has limited controllability. (b) LLM-based planner: Produces linguistic descriptions and controls, offering high interactivity and interpretability at the expense of inference speed. (c) AsyncDriver: While leveraging the reasoning capabilities of LLM, a balance between performance and inference speed is achieved through asynchronous control.

adapt to the planner’s predicted trajectories, thus necessitating that the model exhibits stronger predictive accuracy and bias correction capabilities.

As illustrated in Fig.1(a), current learning-based real-time motion planning frameworks [13, 18, 20, 24, 32, 33] typically utilize vectorized map information as input and employ a decoder to predict trajectories. As purely data-driven methods, they are particularly vulnerable to long-tail phenomena, where their performance can significantly degrade in rare or unseen scenarios [6]. Moreover, while some rule-based strategies exist, their manual crafting of rules are found to be inadequate for capturing the entirety of potential complex scenarios, resulting in driving strategies that tend towards extremes either excessive caution or aggression. Furthermore, both learning-based and rule-based planning frameworks suffer from low controllability, which raises concerns regarding the safety and reliability of such systems in dynamic environments.

Recently, the considerable potential of Large Language Models (LLMs), including GPT-4 [1] and Llama2 [38], has been extensively explored within the realm of autonomous driving. Their extensive pre-training on large-scale datasets has established a robust foundation for comprehending traffic rules and scenarios. Consequently, LLM-based planners have demonstrated superior performance in scene analysis, reasoning, and human interaction, heralding new prospects for enhancing the interpretability and controllability of motion planning [9, 46, 48]. Nonetheless, as shown in Fig.1(b), these models frequently encounter several of these specific challenges: 1) The scene information is described through language, which could be constrained by the permissible input token length, making

it challenging to encapsulate complex scene details comprehensively and accurately [28, 29, 34, 44]. 2) Prediction via linguistic outputs entails either directly issuing high-level commands that are then translated into control signals, potentially leading to inaccuracies, or outputting trajectory points as floating-point numbers through language, a task at which LLMs are not adept [22, 29, 45]. 3) Prevalent frameworks primarily utilize LLMs as the core decision-making entity. While this strategy offers advantages in performance, the inherently large number of parameters in LLMs results in a noticeable decrease in inference speed relative to real-time planners, presenting substantial obstacles to their real-world implementation.

In this work, we introduce AsyncDriver, a novel asynchronous LLM-enhanced framework for closed-loop motion planning. As depicted in Fig.1(c), this method aligns the modalities of vectorized scene information and series of routing instructions, fully leveraging the considerable capabilities of LLM for interpreting instructions and understanding complex scenarios. The Scene-Associated Instruction Feature Extraction Module extracts high-level instruction features, which are then integrated into the real-time planner through the proposed Adaptive Injection Block, significantly boosting prediction accuracy and ensuring finer trajectory control. Moreover, our approach preserves the architecture of the real-time planner, allowing for the decoupling of inference frequency between LLM and the real-time planner. By controlling the asynchronous intervals of inference, it significantly enhances computational efficiency and alleviates the additional computational cost introduced by LLM. Furthermore, the wide applicability of our proposed Adaptive Injection Block ensures that our framework can be seamlessly extended to any transformer-based real-time planner, underscoring its versatility and potential for broader application.

To summarize, our paper makes the following contributions:

- We propose AsyncDriver, a novel asynchronous LLM-enhanced framework, in which the inference frequency of LLM is controllable and can be decoupled from that of the real-time planner. While maintaining high performance, it significantly reduces the computational cost.
- We introduce the Adaptive Injection Block, which is model-agnostic and can easily integrate scene-associated instruction features into any transformer-based real-time planner, enhancing its ability in comprehending and following series of language-based routing instructions.
- Compared with existing methods, our approach demonstrates superior closed-loop evaluation performance in nuPlan’s challenging scenarios.

2 Related Work

2.1 Motion Planning For Autonomous Driving

The classic modular pipeline for autonomous driving includes perception, prediction, and planning. In this framework, the planning stage predict a future

trajectory based on the perception outputs, then executed by the control system. This architecture, widely adopted in industry frameworks like Apollo [3], contrasts with end-to-end approaches [16, 17] by enabling focused research on individual tasks through well-defined data interfaces between modules.

Autonomous driving planners can be mainly categorized into rule-based and learning-based types. Rule-based planners [2, 10, 11, 21, 23, 39, 40] rely on predefined rules for determining the vehicle’s trajectory, such as maintaining a safe following distance and obeying traffic signals. For instance, IDM [39] ensures a safe distance from the leading vehicle by calculating an appropriate speed based on braking and stopping distances. PDM [10] builds on IDM by selecting the highest-scoring IDM proposal as the final trajectory, achieving state-of-the-art performance in the nuPlan Challenge 2023 [4]. However, rule-based planners often struggle with complex driving scenarios beyond their predefined rules.

Learning-based planners [13, 18, 20, 24, 32, 33] aim to replicate human expert driving trajectories using imitation learning or offline reinforcement learning from large-scale datasets. However, they face limitations due to the scope of the datasets and model complexity, leaving substantial room for improvement in areas like routing information comprehension and environmental awareness.

2.2 LLM For Autonomous Driving

The rapid advancement of Large Language Models has been noteworthy. These models, including GPT-4 [1] and Llama2 [38], have been trained on extensive textual datasets and exhibit exceptional generalization and reasoning abilities. A growing body of research has explored the application of LLMs’ decision-making capacities to the domain of autonomous driving planning [5, 7, 8, 12, 14, 19, 25–29, 31, 34–37, 41–45, 47].

Some efforts [12, 28, 29, 44] have explored integrating scene information, including the ego vehicle’s status and information about obstacles, pedestrians, and other vehicles into LLMs using linguistic modalities for decision-making and explanations. These approaches face limitations due to finite context length, making it challenging to encode precise information for effective decision-making and reasoning. To overcome these constraints, multi-modal strategies such as DrivingWithLLM [7], DriveGPT4 [45], and RAGDriver [47] have been developed. These methods align vectorized or image/video modalities with linguistic instructions for a more comprehensive interpretation of driving scenarios. However, using language to express control signals has its limitations. DrivingWithLLM outputs high-level commands in linguistic expressions, improving QA interaction but reducing the fidelity of translating complex reasoning into precise vehicle control. DriveGPT4 expresses waypoints through language, showing strong open-loop performance but lacking closed-loop simulation evaluation.

Furthermore, some efforts [34, 35] focus on closed-loop evaluation by connecting low-level controllers or regressors behind large language models for precise vehicle control. LMDrive [35] uses continuous image frames and navigation instructions for closed-loop driving but requires complete LLM inference at each planning step. LanguageMPC [34] employs LLMs to obtain Model Predictive

Control parameters, achieving control without training. However, these methods necessitate serial language decoding or full LLM inference at each planning step, challenging real-time responsiveness and limiting practical deployment.

In our approach, we shift from using LLMs for direct language output to enhancing real-time learning-based planners. This strategy improves environmental comprehension and allows LLMs and real-time planners to operate independently at different inference rates. This decoupling reduces LLM inference latency, facilitating real-world deployment.

3 Data Generation

The nuPlan [4] dataset is the first large-scale benchmark for autonomous driving planning, comprising 1,200 hours of real-world human driving data from Boston, Pittsburgh, Las Vegas, and Singapore. To support various training stages, we developed pre-training and fine-tuning datasets from the nuPlan *Train* and *Val* sets, focusing on 14 official [30] challenging scenario types.

3.1 Pre-training Data Generation

To enhance LLM’s understanding of instructions in autonomous driving, we created a dataset of language-based QAs, aligning with LLM’s native modality to better grasp instruction semantics, which includes *Planning-QA* and *Reasoning1K*, with sample datasets provided in the supplementary material.

Planning-QA is created using a rule-based approach for scalability. It is designed to enhance the LLM’s understanding of the relationships among waypoints, high-level instructions, and control. In this context, waypoints are arrays of points, high-level instructions are composed of velocity commands (*stop*, *accelerate*, *decelerate*, *maintain speed*) and routing commands (*turn left*, *turn right*, *go straight*), and control involves velocity and acceleration values. Planning-QA includes six types of questions, each focusing on the conversion between waypoints, high-level instructions, and control.

Reasoning1K includes 1,000 pieces of data generated by GPT-4, beyond merely providing answers, it further supplements the reasoning and explanation based on the scene description and is used for mixed training with Planning-QA.

3.2 Fine-tuning Data Generation

To further achieve multimodal understanding and alignment, we constructed a fine-tuning dataset based on 10,000 scenarios, capturing one frame every 8 seconds, resulted in a training set of 180,000 frames and a validation set of 20,000 frames, each incorporating both vectorized map data and linguistic prompts. Importantly, the scenario type distribution in both training and validation datasets matches the distribution of the entire nuPlan trainval dataset.

For the extracted vectorized scene information, similar to [18], ego information and 20 surrounding agent information over 20 historical frames, in addition to global map data centered around the ego are involved.

LLM’s prompt is comprised of two parts: system prompt and series of routing instructions. Concerning routing instructions, a rule-based approach is employed to transform the pathway into a series of instructions enhanced with distance information. Regarding training dataset preparation, the ego vehicle’s ground truth trajectory over the ensuing 8 seconds is harnessed as the pathway for routing instruction generation. During simulation, based on the observation of the current scene, a pathway that adheres to a specified maximum length is found through a hand-crafted method as a reference path for instruction generation.

4 Methodology

As illustrated in Fig. 2, we introduce the asynchronous LLM-enhanced closed-loop framework, AsyncDriver, which mainly includes two components: 1) The Scene-Associated Instruction Feature Extraction Module; 2) The Adaptive Injection Block. Additionally, due to our framework’s design, the inference frequency between the LLM and the real-time planner could be decoupled and regulating by asynchronous interval, which markedly enhancing inference efficiency.

Within this section, we present the Scene-Associated Instruction Feature Extraction Module (Section 4.1), detail the design of Adaptive Injection Block (Section 4.2), discuss the concept of Asynchronous Inference (Section 4.3) and outline the training details employed (Section 4.4).

4.1 Scene-Associated Instruction Feature Extraction Module

Multi-modal Input In each planning iteration, the vectorized scene information is acquired from the simulation environment. Analogous to the approach employed by GameFormer [18], historical trajectory and state information of both the ego and other agents are extracted, alongside global map data. Vectorized scene information for the real-time planner is provided in the same manner. All vector data are relative to the position of the ego. Subsequently, through the processing by the Vector Map Encoder and Map Adapter, we derive map embeddings. These map embeddings, along with language embeddings, are then fed into the Llama2-13B backbone to obtain the final hidden features $h = \{h_0, h_1, \dots, h_{-1}\} \in \mathbb{R}^{N_h \times Dim}$.

Alignment Assistance Module To grasp the essence of routing instructions while maintaining a fine-grained comprehension of vectorized scene information for enhanced extraction of scene-associated high-level instruction features, we employ the Alignment Assistance Module to facilitate the alignment of multi-modal input. Concretely, we have pinpointed five critical scene elements essential to the autonomous driving process for multi-task prediction, which is implemented by five separate 2-layer MLP prediction heads. About the current states

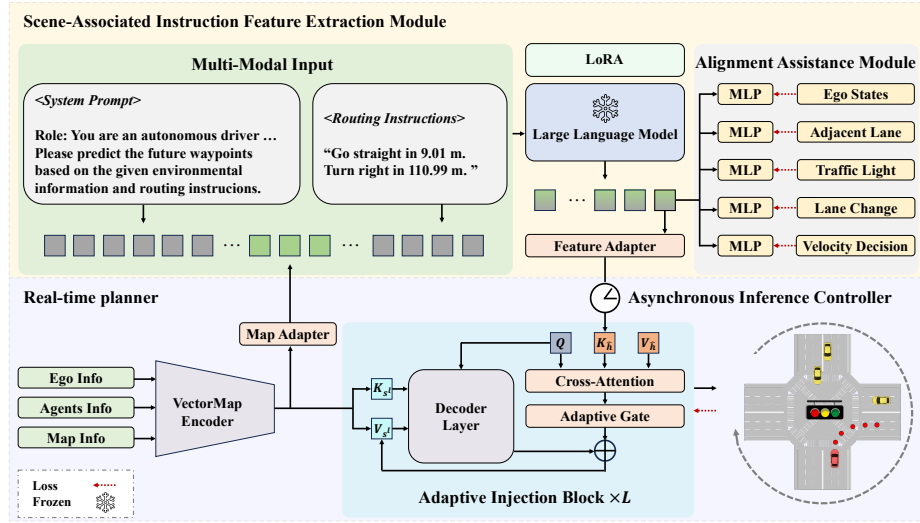


Fig. 2: Overview of our proposed AsyncDriver framework. Scene information, together with routing instructions, is encoded through the Scene-Associated Instruction Feature Extraction Module. Subsequently, the Adaptive Injection Block asynchronously enhances the features of the real-time planner, facilitating closed-loop control for autonomous vehicles. The Alignment Assistance Module is exclusively employed for multi-modality alignment during training.

of the ego vehicle, we perform regression to estimate the vehicle’s velocity and acceleration along the X and Y axes. For map information, we undertake classification tasks to identify the existence of adjacent lanes on both the left and right sides and to assess the status of traffic lights relevant to the current lane. Additionally, with a view towards future navigation strategies, we classify the requirement for lane changes in upcoming trajectories and identify future velocity decision, which includes options *acceleration*, *deceleration*, and *maintaining current speed*. It is worth noting that the Alignment Assistance Module is only used to assist multi-modal alignment in the training phase and does not participate in the inference stage.

4.2 Adaptive Injection Block

We adopt the decoder structure of [18] as our basic decoder layer, facilitating the adaptive integration of scene-associated instruction features by evolving the conventional transformer-based decoder layer into an Adaptive Injection Block.

Specifically, the hidden feature of the last token h_{-1} is projected via the feature adapter and subsequently fed into Adaptive Injection Block.

$$\hat{h} = \text{Linear}(h_{-1}) \quad (1)$$

Within the Adaptive Decoder Block, the foundational decoder architecture of the real-time planner is elegantly extended to ensure that the query in each layer not only preserves the attention operation intrinsic to the original scene information but also engages in cross-attention with scene-associated instruction features, thereby incorporating instructional guidance into the prediction process. Afterwards, the updated instruction-enhanced query feature is modulated by the learnable adaptive gate, which is initialized by zero and reintegrated into the original attention output of the decoder layer. The adaptive injection process of the l -th decoder block can be formulated as follows:

$$s^{l+1} = g \cdot \text{softmax}\left(\frac{QK_h^T}{\sqrt{C}}\right)V_h + \text{softmax}\left(\frac{QK_{s^l}^T}{\sqrt{C}}\right)V_{s^l} \quad (2)$$

where g is the value of adaptive gate, Q denotes query in original decoder layer, K_i and V_i represent key and value respectively of feature i , and s^l notes the scene feature of the l -th decoder layer.

The proposed adaptive injection method not only maintains the original decoder layer’s ability to process complete scene information within the real-time planner but also enhances the planner’s understanding and compliance with a series of flexible linguistic instructions. This advancement allows for the production of more refined and controllable predictions. It is worth noting that due to the simple yet effective design of our Adaptive Injection Block, it can be seamlessly integrated into any transformer-based architecture, thereby affording our approach the flexibility to be adapted to other real-time planner frameworks.

4.3 Asynchronous Inference

Our design leverages LLM to guide the real-time planner, significantly enhancing its performance through series of flexibly combined linguistic instructions without compromising its structural integrity. This method facilitates controlled asynchronous inference, effectively decoupling the inference frequencies of the LLM and the real-time planner, thereby LLM is not required to process every frame. During asynchronous intervals, the previously derived high-level instruction features continue to guide the prediction process of the real-time planner, which significantly boosts the inference efficiency and reduces the computational cost introduced by LLM. Notably, our framework accommodates a series of flexibly combined routing instructions, capable of delivering long-term, high-level routing insights. Therefore, even amidst asynchronous intervals, prior high-level features could still offer effective guidance, reinforcing the performance robustness throughout LLM inference intervals.

Experimental results reveal that our architecture maintains near-robust performance when the asynchronous inference interval of LLM is extended. By controlling the LLM to perform inference every 3 frames can achieve a reduction in inference time of nearly 40%, with only a minimal accuracy loss of about 1%, which demonstrates the efficacy of our approach in striking an optimal balance between accuracy and inference speed. For a more comprehensive exploration of experimental results and their analysis, please refer to Section 5.2.

4.4 Training Details

During the pre-training stage, the entirety of Reasoning1K, augmented with 1, 500 samples randomly selected from Planning-QA, was utilized to train LoRA. This process enabled the LLM to evolve from a general-purpose large language model into one specifically optimized for autonomous driving. As a direct outcome of this focused adaptation, the LLM has become adept at understanding instructions more accurately within the context of motion planning.

During the fine-tuning stage, since the architectures of VectorMap Encoder and Decoder are preserved, we load weights of the real-time planner pre-trained on the same dataset to enhance training stability. The total loss of the fine-tuning stage is comprised of Alignment Assistance Loss and Planning Loss. The former is partitioned into five components: $l1$ loss for 1) ego velocity and acceleration prediction $\tilde{x}_{va} \in \mathbb{R}^4$, cross-entropy loss for 2) velocity decision prediction $\tilde{x}_{dec} \in \mathbb{R}^3$ and 3) traffic light state prediction $\tilde{x}_{traf} \in \mathbb{R}^4$, binary cross-entropy loss for 4) adjacent lane presence prediction $\tilde{x}_{adj} \in \mathbb{R}^2$ and 5) lane change prediction $\tilde{x}_{chg} \in \mathbb{R}$. The complete Alignment Assistance Loss can be expressed as follows, where \tilde{x} and x represent prediction and ground truth respectively:

$$L_{align} = L_1(\tilde{x}_{va}, x_{va}) + CE(\tilde{x}_{dec}, x_{dec}) + CE(\tilde{x}_{traf}, x_{traf}) + BCE(\tilde{x}_{adj}, x_{adj}) + BCE(\tilde{x}_{chg}, x_{chg}) \quad (3)$$

Following [18], the planning loss comprises two parts: 1) Mode prediction loss. m different modes of trajectories of neighbor agents are represented by Gaussian mixture model (GMM). For each mode, at any given timestamp t , its characteristics are delineated by a mean μ^t and covariance σ^t forming a Gaussian distribution. The best mode m^* is identified through alignment with the ground truth and refined via the minimization of negative log-likelihood. 2) Ego Trajectory Prediction loss. Future trajectory points of ego vehicle are predicted and are refined by $l1$ loss. Consequently, the planning loss is as follows:

$$L_{plan} = \sum_t L_{NLL}(\tilde{\mu}_{m^*}^t, \tilde{\sigma}_{m^*}^t, \tilde{p}_{m^*}, \tilde{s}_t) + \sum_t L_1(\tilde{s}_t - s_t) \quad (4)$$

where $\tilde{\mu}_{m^*}^t, \tilde{\sigma}_{m^*}^t, \tilde{p}_{m^*}, \tilde{s}_t$ represents the predicted mean, covariance, probability, and position respectively, corresponding to the best mode m^* at timestamp t , and s_t indicates the ground truth position at timestamp t .

In summary, the complete loss of fine-tuning stage is formulated as:

$$L = L_{align} + L_{plan} \quad (5)$$

5 Experiments

5.1 Experimental Setup

Evaluation Settings In accordance with the nuPlan challenge 2023 [30] settings, we selected 14 official challenging scenario types for training and eval-

Table 1: Evaluation on nuPlan Closed-Loop Reactive Challenges on *Hard20* split. The best results are highlighted in **bold**, while the second-best results are underscored with an underline for clear distinction. *Score*: final score in average. *Drivable*: drivable area compliance. *Direct.*: driving direction compliance. *Comf.*: ego is comfortable. *Prog.*: ego progress along expert route. *Coll.*: no ego at-fault collisions. *Lim.*: speed limit compliance. *TTC*: time to collision within bound.

Method	Score	Drivable	Direct.	Comf.	Prog.	Coll.	Lim.	TTC
UrbanDriver [33]	35.35	75.53	97.12	98.56	85.23	55.21	81.62	47.84
GCPGP [13]	36.85	81.29	98.20	77.33	46.96	72.30	97.92	68.34
IDM [39]	53.07	84.94	98.02	83.15	64.79	74.01	96.38	60.57
GameFormer [18]	62.05	93.54	98.74	83.15	66.27	86.02	98.19	<u>74.55</u>
PDM-Hybrid [10]	64.05	95.34	99.10	75.98	67.93	87.81	99.57	<u>72.75</u>
PDM-Closed [10]	64.18	<u>95.69</u>	<u>99.10</u>	77.06	<u>68.20</u>	87.81	99.57	73.47
AsyncDriver	<u>65.00</u>	94.62	98.75	83.15	67.13	85.13	98.15	73.48
AsyncDriver*	67.48	96.77	99.10	<u>83.87</u>	66.30	<u>87.63</u>	<u>98.24</u>	76.70

Table 2: Scores per scenario types in evaluation on nuPlan Closed-Loop Reactive Challenges on *Hard20* split. The best results are highlighted in **bold**, while the second-best results are underscored with an underline for clear distinction. Types 0-13 represent the 14 official scenario types of the nuPlan challenge 2023 [30], with specific details provided in the supplementary materials.

Methods	type0	type1	type2	type3	type4	type5	type6	type7	type8	type9	type10	type11	type12	type13
UrbanDriver [33]	69.39	15.78	44.59	7.42	13.7	27.14	0.00	19.44	20.8	23.61	68.33	93.16	33.78	56.39
GCPGP [13]	59.50	35.91	33.6	29.33	42.84	17.24	4.86	32.33	8.22	36.23	71.32	80.46	36.19	23.61
IDM [39]	70.69	44.84	<u>91.54</u>	54.08	50.22	41.71	4.76	53.97	37.53	60.33	83.97	93.03	45.77	12.44
GameFormer [18]	84.32	65.78	83.62	49.03	71.79	36.8	0.00	51.76	55.03	77.24	82.83	98.24	49.41	56.16
PDM-Hybrid [10]	87.68	69.61	87.20	49.95	82.80	41.32	4.23	54.98	51.72	<u>82.95</u>	80.37	<u>98.40</u>	37.77	<u>71.99</u>
PDM-Closed [10]	<u>87.67</u>	<u>70.93</u>	87.20	49.95	82.80	41.25	4.22	53.53	51.57	82.96	80.37	98.40	39.95	72.04
AsyncDriver	83.53	67.24	83.14	62.89	<u>83.28</u>	<u>49.26</u>	<u>5.94</u>	<u>62.53</u>	65.96	64.86	84.88	96.62	<u>49.60</u>	54.35
AsyncDriver*	83.12	74.04	91.82	<u>62.42</u>	85.26	53.51	6.01	65.26	<u>57.31</u>	77.16	<u>84.02</u>	97.56	62.18	49.32

uation. While nuPlan [4] includes 757,844 scenarios, most simple scenarios are insufficient for critical planner performance assessment, and the vast data volume extends evaluation times. We chose the *Hard20* dataset by randomly selecting 100 scenarios per type from the test set, then using the PDM [10] planner (nuPlan 2023 champion) to retain the 20 lowest-scoring scenarios per type, resulting in a test set of 279 scenarios.

Implementation Details Regarding implementation details, all experiments were conducted in the closed-loop reactive setting, where agents in scenarios could be equipped with an IDM [39] Planner, enabling them to react to ego vehicle’s maneuvers. The simulation frequency is $10Hz$, at each iteration, the predicted trajectory has a time horizon of $8s$. We follow the closed-loop metrics proposed in nuPlan challenge, which is detailed in the supplementary material. For model settings, our AsyncDriver is built based on Llama2-13B [38], LoRA

[15] was configured with $R = 8$ and $\alpha = 32$. We use the AdamW optimizer and warm-up with decay scheduler with learning rate 0.0001.

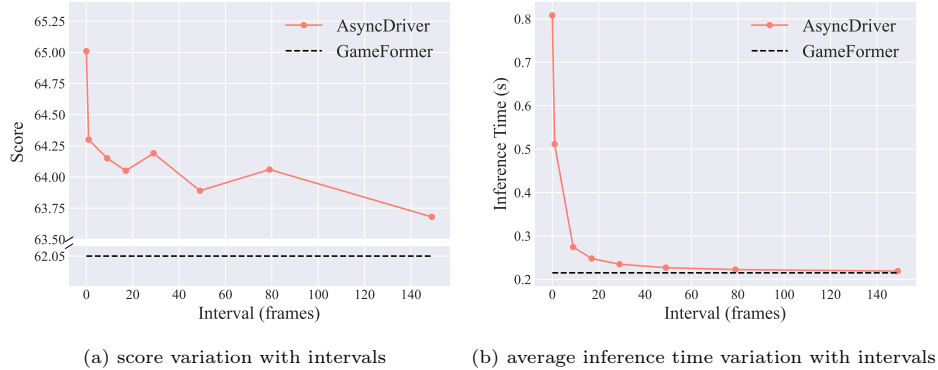


Fig. 3: Asynchronous Inference. Evaluation of expanding the inference interval to [1, 9, 17, 29, 49, 79, 149] between the LLM and the real-time planner, executing asynchronous inference. Inference time measured on GPU Tesla A30.

5.2 Main Results

Hard20 Evaluation As illustrated in Tab. 1, our approach AsyncDriver achieved the highest performance on *Hard20* compared with existing planners, leading to an improvement of 4.6% over GameFormer [18] about 2.95 in score, even surpassing the current SOTA rule-based planners. For fair comparison, given the significant impact of trajectory refinement and alignment in closed-loop evaluations, we adapt the PDM [10] scorer to our AsyncDriver (denoted as AsyncDriver*), which lead to an improvement of 5.3% and 5.1% over PDM-Hybrid [10] and PDM-Closed [10] respectively, equivalent to approximately 3.43 and 3.30 in score, and an 8.7% increase (approximately 5.43 in score) over the learning-based planner GameFormer. From a different perspective, Tab. 2 illustrates the scores of each individual scenario type on the *hard20* split, as well as a comparison with existing planners. It is evident that our solution has delivered exceptional results in the majority of scenario types.

Quantitative results show that the high-level features extracted by our Scene-Associated Instruction Feature Extraction Module significantly enhance real-time planners’ performance in closed-loop evaluation. Detailed metrics reveal that our approach improves drivable area performance by 3.23 points compared to GameFormer, demonstrating superior capability in identifying and navigating viable driving spaces due to advanced scene contextual understanding. Additionally, AsyncDriver* outperforms PDM in Time to Collision (TTC) metrics by 4.39%, approximately 3.23 points, indicating enhanced predictive accuracy,

which is crucial for ensuring safer driving by effectively forecasting and reducing the potential collision scenarios.

Asynchronous Inference We contend that, particularly for generalized high-level instructions, there exhibits a notable similarity within frames of short intervals. Consequently, given its role in extracting these high-level features, the LLM does not require involvement in the inference process for each frame, which could markedly enhance the inference speed. To explore this, experiments were designed to differentiate the inference frequency of the LLM and real-time planners, and during each LLM inference interval, the previous instruction features are employed to guide the predicted process of the real-time planner. As depicted in Fig. 3, the performance of our approach demonstrates remarkable robustness as the planning interval of the LLM increases, which suggests that LLM is capable of providing a long-term high-level instructions. We observed that even with an interval of 149 frames, meaning only one inference is made within a scenario, it still surpasses GameFormer by more than 1.0 point, while the inference time is nearly at the real-time level. As the inference interval increases, the required inference time drops dramatically, while accuracy remains almost stable. Therefore, by employing a strategy of dense training with asynchronous inference, our method achieves an optimal balance between accuracy and inference speed.

Instruction Following Fig. 4 shows the reactions of our method to different routing instructions, demonstrating its capability in instruction following. Fig. 4a illustrates the outcomes predicted when the scene employs conventional routing instructions. We note that the ego vehicle decelerates slightly, a maneuver that reflects the common sense of slowing down for curves. Nonetheless, given the open road conditions, the ego vehicle sustains a comparatively high velocity. In contrast, Fig. 4b depicts the scenario where *stop* serves as the routing instruction. Remarkably, even without the presence of external obstacles, the ego vehicle promptly executes a braking response to the command, reducing its speed from $10.65m/s$ to $1.06m/s$ within a mere 6 seconds. Consequently, it is evident that our AsyncDriver can function as a linguistic interaction interface, providing the ability of precisely interpreting and following human instructions to circumvent anomalous conditions.

5.3 Ablation Study

In this section, we explore the necessity of LLM and investigate the effectiveness of individual components in AsyncDriver.

Necessity of LLM We conducted experiments by replacing the LLM with transformer blocks of different dimensions (256 and 5120), incorporating learnable routing instruction embeddings. Meanwhile, the Alignment Assistance Module and Adaptive Injection Block remained unchanged. The results, shown in

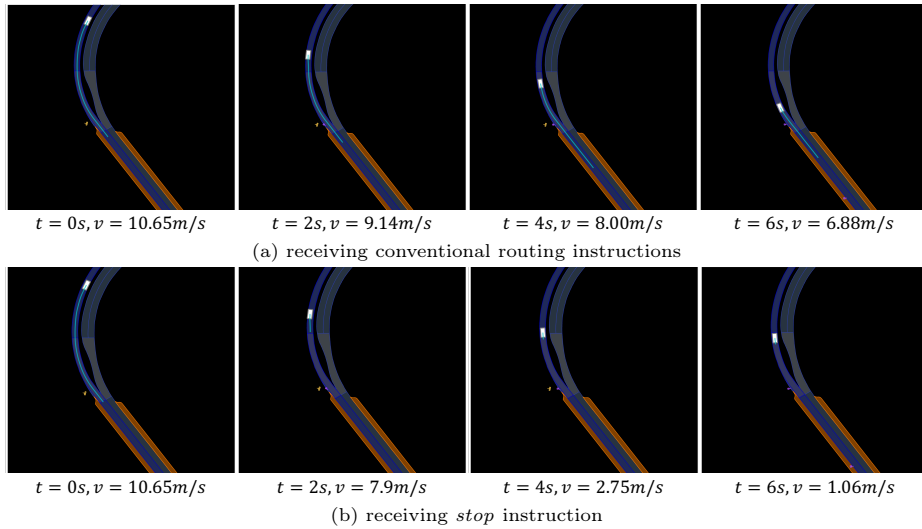


Fig. 4: Visualization of AsyncDriver following human instruction. The light blue line represents ego’s trajectory for the next 8 seconds. It contrasts the planning trajectories of the ego receiving conventional routing instructions against a forced *stop* instruction.

Tab. 3, indicate that despite a 20-fold increase in the number of transformer parameters, the performance only marginally improved from 63.27 to 63.59. In contrast, our AsyncDriver achieved a performance of 65.00, highlighting the significant impact of pretrained knowledge from LLM.

Ablation of Components Integrating a simple MLP as a prediction head after the LLM for planning significantly degraded the performance, indicating that simple trajectory regression cannot effectively align multi-modal information, thus failing to leverage the LLM’s knowledge for scene reasoning. We replaced the MLP with a real-time planner and progressively added four structures: (i) Adaptive Injection Block, (ii) Alignment Assistance Module, (iii) LoRA, and (iv) pre-trained LoRA. As shown in Tab. 4, each module improved performance, with the Alignment Assistance Module and pre-trained LoRA weights contributing the most, yielding score increases of 0.94 and 0.97, respectively.

6 Conclusions

In this paper, we introduce AsyncDriver, a new asynchronous LLM-enhanced, closed-loop framework for autonomous driving. By aligning vectorized scene information with a series of routing instructions to form multi-modal features, we fully leverage LLM’s capability for scene reasoning, extracting scene-associated instruction features as guidance. Through the proposed Adaptive Injection Block,

Table 3: Replacing LLM with non-pretrained cross attention. Utilize map information and learnable instruction embeddings to perform cross-attention, replacing the features generated by the LLM in the Scene-Associated Instruction Feature Extraction Module.

Hidden Feature Dimensions	Instruction Embedding	LLM	Score
256	✓		63.27
5120	✓		63.59
5120		✓	65.00

Table 4: Component ablation study. MLP, RT-Planner, Ada, Align, LoRA, and LoRAPre represent i) direct regression of waypoints using MLP, ii) integration of a real-time planner, iii) Adaptive Injection Block, iv) Alignment Assistance Module, v) incorporation of LoRA, and vi) pre-trained LoRA with *Reasoning1K*, respectively.

MLP	RT-Planner	Ada	Align	LoRA	LoRAPre	Score
✓						33.91
	✓					62.01
	✓	✓				62.84
	✓	✓	✓			63.78
	✓	✓	✓	✓		64.03
	✓	✓	✓	✓	✓	65.00

we achieve the integration of series of routing information into any transformer-based real-time planner, enhancing its ability to understand and follow language instructions, and achieving outstanding closed-loop performance in nuPlan’s challenging scenarios. Notably, owing to the structural design of our method, it supports asynchronous inference between the LLM and the real-time planner. Experiments show that our approach significantly increases inference speed with minimal loss in accuracy, reducing the computational costs introduced by LLM.

Broader Impacts And Limitations. Should the method prove successful, the proposed asynchronous inference scheme could significantly enhance the prospects for integrating LLMs into the practical application within the autonomous driving sector. Nevertheless, while this research has employed LLMs, it falls short of substantiating their generalization properties for the planning task. Future endeavors aim to rigorously assess the generalization and transfer potential of LLMs in in vectorized scenarios.

Acknowledgements

This research is supported in part by the National Science and Technology Major Project (No. 2022ZD0115502), the National Natural Science Foundation of China (No. 62122010, U23B2010), Zhejiang Provincial Natural Science Foundation of China (No. LDT23F02022F02), Beijing Natural Science Foundation (No. L231011), Beihang World TOP University Cooperation Program, and Lenovo Research.

Appendix

In this supplementary material, we first present the templates for QAs and prompts of pre-training and fine-tuning data (Appendix A). Then, we provide detailed metric information for our closed-loop evaluation (Appendix B), as well as the specific 14 scenario types defined in nuPlan challenges [30] (Appendix C). In the end, we report additional quantitative results conducted to further substantiate the efficacy of our approach (Appendix D).

A Data Templates

A.1 Pre-training Data

Planning-QA We assessed the capabilities of Llama2-13B [38] via a zero-shot methodology and discovered that its extensive pre-training data provides a solid foundation in traffic rule comprehension. However, its limited mathematical prowess poses challenges in grasping and deducing the connections between instructions and numerical expressions. To address this, we introduced a language-based *Planning-QA* dataset aimed at transitioning LLM from a general model to a specialized model adept in autonomous driving planning. This enhancement focuses on refining its capability in instruction interpretation and reasoning.

Concretely, we delineated the level of autonomous driving planning into three granularities: 1) high-level instructions: formulated through velocity commands including *stop*, *accelerate*, *decelerate*, *maintain speed*, and routing commands including *turn left*, *turn right*, *go straight*, 2) control: assessing the values of velocity and acceleration, 3) and waypoint: encompassing a series of points. Six question types were devised to articulate the transitional relationships across the *high-level instructions* - *control* - *waypoint* spectrum, and each QA-pair is adapted based on log data from nuPlan [4]. Fig. S1a illustrates the universal system prompt template applicable to all questions, whereas Fig. S1b-S1g display specific examples for each question type alongside their respective answer, substituting **<Question>** and **<Answer>** within the system prompt.

- Input:
Role: You are now an autonomous driving driver, you need to answer questions based on the given high-level instructions, control or waypoints information.
Coordinate: Your current coordinate is at (0,0), the positive direction of the x-axis is to the front, and the positive direction of the y-axis is to the left. The waypoints are represented as a series of equally time-spaced points, with the time interval between two adjacent points being 0.5 s.
Question: <Question>
Final Answer:

- Target:
 <Answer>

(a) system prompt template for Planning-QA dataset

<Question>
 Given the waypoints $[[1.543 -0.123] [4.337 -0.251] [7.463 -0.469] [10.919 -0.8]]$ and the high-level instructions **turn right for 9.402 m, during the way, we decelerate**, are they consistent? If not, what should the corresponding high-level instructions be? And what exactly is different about the high-level instructions?

<Answer>
- Positive answer:
 The high-level instructions corresponding to the given waypoints is **turn right for 9.402 m, during the way, we decelerate**, which is consistent with the given high-level instructions.

- Negative answer:
 The high-level instructions corresponding to the given waypoints is **go straight for 9.402 m, during the way, we accelerate**, which is not consistent with the given high-level instructions **turn right for 9.402 m, during the way, we decelerate**. The given high-level instructions requires a **turn right** and a **decelerate**, but the waypoints correspond to **go straight** and **accelerate**.

(b) waypoints - high-level instructions

<Question>
 The driving waypoints $[[1.493 -0.574] [4.073 -0.577] [6.653 -0.58] [9.233 -0.583]]$, initial speed **5.16 m/s**, accelerating time **1.5 s** and acceleration **1.05 m/s**2** are known. Known that acceleration is a fixed value, does the given acceleration matches with the waypoints? If not, what should the real acceleration value be?

<Answer>
- Positive answer:
 Through the given waypoints and initial velocity, the acceleration corresponding to the waypoints is **1.05 m/s**2**, which is consistent with the given acceleration.

- Negative answer:
 Through the given waypoints and initial velocity, the acceleration corresponding to the waypoints is **0.1 m/s**2**, which is **smaller (resp. greater)** than the given acceleration **1.05 m/s**2**.

(c) waypoints - control

<Question>
 Driving following the lane, where the centerline ahead is $[[1.543 -0.123] [1.789 -0.132] [2.035 -0.141] [2.281 -0.151] [2.526 -0.161] [2.772 -0.172] \dots [13.058 -1.053] [13.302 -1.084] [13.546 -1.116]]$. And the initial speed **11.721 m/s**, acceleration **1.318 m/s**2**, driving time **0.5 s** are known, what should the future waypoints be?

<Answer>
 Based on the given input, the waypoints in the future **0.5 s** is $[[1.543 -0.123] [7.558 -0.476]]$.

(d) high-level instructions - waypoint

<Question>
 Known that the initial speed is **5.305 m/s**. Can we stop in **3.0 s** if the acceleration is **-0.402 m/s**2**?

<Answer>
- Positive answer:
 Based on the given input, we could stop in **3.0 s**.

- Negative answer:
 Based on the given input, we could not stop in **3.0 s**.

(e) high-level instructions - control

<Question>
 Does the waypoints $[[1.482 -0.853] [4.136 -0.853] [6.789 -0.848] [9.442 -0.85]]$ consistent with the condition that driving follow the lane $[[1.482 -0.853] \dots [11.218 -0.855] [11.429 -0.856] [11.641 -0.857] [11.853 -0.858]]$, where the initial speed is **5.307 m/s**, acceleration is **1.7 m/s**2**? If not, what should the real acceleration be? If it does, how long is the driving time?

<Answer>
- Positive answer:
 The waypoint is consistent with the given input. And the driving time corresponding to the waypoints **1.5 s**.

- Negative answer:
 The waypoint is not consistent with the given input. The acceleration corresponding to the given input is **0.1 m/s**2**, but the given acceleration is **1.7 m/s**2**.

(f) control - waypoint

<Question>
 Given the initial speed **1.033 m/s** and acceleration **-0.007 m/s**2**, and driving along the centerline **[[1.413 -0.19] [1.668 -0.187] [1.922 -0.183] ... [13.123 -0.012] [13.378 -0.013] [13.632 -0.015] [13.887 -0.017]]**, according to the current state, what should the corresponding high-level instructions be? Is it consistent with the given high-level instructions **turn left for 115.5 m, during the way, we stop**?

<Answer>
- Positive answer:
 Based on the given input, the high-level instructions should be **turn left for 115.5 m, during the way, we stop**, which is consistent with the given high-level instructions.

- Negative answer:
 Based on the given input, the high-level instructions should be **go straight for 115.5 m, during the way, we decelerate**, which is not consistent with the given high-level instructions **turn left for 115.5 m, during the way, we stop**. The given high-level instructions requires a **turn left** and a **stop**, but the waypoints correspond to **go straight and decelerate**.

(g) control - high-level instructions

Fig. S1: Six question types were devised to articulate the transitional relationships across the *high-level instructions* - *control* - *waypoints* spectrum. All data are generated based on logs from nuPlan, with the red parts being subject to change based on actual data. Some data have both positive and negative answers, which are both displayed in the corresponding templates. The waypoints are abbreviated due to space limitations.

Reasoning1K Additionally, we have crafted 1,000 QA-pairs using GPT-4, tailored to tasks that require not just decision-making but also in-depth reasoning. Each sample includes a question that sets the context, provides scene descriptions, outlines considerations based on traffic rules, details the anchor trajectory from real-time planners, and specifies requirements for the answers, while the answer delivers trajectory predictions along with the decisions and the underlying thought process. By training with mixed of *Reasoning1K* and *Planning-QA*, we have substantially enriched the dataset’s diversity and complexity. This approach aims to bolster LLM’s ability to deduce answers through logical reasoning, seamlessly integrating traffic rules with detailed, scenario-based analysis. Fig. S2a and Fig. S2b showcase an example of the input and its corresponding target from the dataset, respectively.

A.2 Fine-tuning Data

The pre-training phase aims to utilize language-based data to bolster the LLM’s understanding of instructions, whereas the fine-tuning phase seeks to further refine this comprehension by aligning it with vectorized scenes. This entails a process characterized by multi-modal inputs and vectorized supervision. Inputs encompass two parts: linguistic prompts and vectorized scene data. The linguistic portion includes fixed system prompts and log-based routing instructions. Within this template, the **<map>** token is substituted with tokens of vectorized scene at the point of input. Instructions are generated from the forthcoming 8 seconds’ logs through a hand-crafted rules, encompassing four instruction categories—*turn left*, *turn right*, *go straight*, and *stop*—paired with pertinent distance details. Notably, the *stop* is only employed when the actual path length for

- Input:
Role: You are now an autonomous driving driver, I will provide you with a predicted future trajectory. Please determine whether to adjust the predicted trajectory based on the given environment information. Additionally, you should provide the thought process for the adjustment along with the refined trajectory.

Context:
 - Trajectories: Trajectories are represented by 16 points. Each point is represented by (x, y). The time interval between two points is 0.5s.

Environment:
 - Speed: Car speed on X-axis is 6.3m/s, car speed on Y-axis is -0.0m/s.
 - Location: Car location is (0.0, 0.0).
 - Acceleration: Car acceleration on X-axis is 1.29m/s², car acceleration on Y-axis is 0.0m/s².
 - Lane: You are in the 1st lane from the left. **There are 1 lanes in total**, which means there are 0 lanes on your left, and 0 lane on your right. **The width of each lane is 3.75m.**
 - Sampled 16 points of the center of the 1st lane from the left.: [(1.46, 0.0) ... (70.47, -21.34)]
 - **Traffic Light: traffic lights of incoming lane connector are: GREEN**
 - **Other Vehicles: There are 0 vehicles or pedestrians near you.**

Traffic Rules:
 1. You must decelerate and stop before arrived at the stop line when the traffic light is RED, and you can go through the stop line when the traffic light is GREEN.
 2. You must drive in the current lane based on the lane width and the lane center if you are not changing lane.
 3. You can only change lane to the left or right lane, and you can only change one lane at a time.
 4. **You can accelerate if there is no car in front of you, but you can not exceed the speed limit of 50.0m/s.**
 5. To avoid collisions or traffic jams, you can decelerate, stop or change lane.
 6. By default, other vehicles will not change lanes on their own.

Inputs:
 - Predicted Ego Future Trajectories in next 8.0s : [(1.46, 0.0), (4.73, 0.47) ... (42.56, 7.91), (43.6, 7.99)]

Outputs:
 - Refined Ego Future Trajectories in next in next 8.0s.
 - Decision: How to adjust the predicted trajectory, such as accelerate, decelerate, stop or change lane, etc.
 - Thought process: Think step by step why the Refined trajectory is better than the predicted trajectory. You can only analysis based on the environment information. Besides, You must contain the follow things:
 1. Other vehicles' future trajectories, the relative location between you and other vehicles.
 2. Traffic rules.

(a) example of input for Reasoning1K

- Target:
 Refined Ego Future Trajectories in next 8.0s : [(4.63, 0.29) ... (53.01, 10.38), (55.96, 10.95)]

Decision: The predicted trajectory needs to be adjusted to align more closely with the center of the lane. This can be achieved by maintaining the current acceleration and speed on X-axis, while slightly increasing the speed on the Y-axis.

Thought Process:
 1. Other Vehicles' Future Trajectories and Relative Location: **There are no other vehicles or pedestrians near us, so we don't need to consider their future trajectories or our relative location to them. This gives us more flexibility in adjusting our trajectory.**
 2. Traffic Rules: **The traffic light is green, so we are allowed to proceed through the intersection without stopping. We are currently in the only lane, so we cannot change lanes.** However, we need to **stay within the lane, which is 3.75m wide.** The predicted trajectory deviates from the center of the lane, which is not ideal. **There is no speed limit constraint as our current speed is well below the limit of 50.0m/s.** Since there are no other vehicles in front of us, we can maintain or even slightly increase our speed if necessary.

Based on these considerations, it's clear that we need to adjust our trajectory to stay closer to the center of the lane. This can be achieved by maintaining our current speed and acceleration on X-axis, while slightly increasing our speed on the Y-axis. This will allow us to move more towards the center of the lane, ensuring a safer and more efficient drive.

(b) example of corresponding target for Reasoning1K

Fig. S2: An example from *Reasoning1K*, where S2a displays the input, and S2b shows the corresponding target. The reasoning-related parts are highlighted in color, with the same color in both input and target representing the cause and effect in the reasoning process respectively.

<p><i>Role: You are now an autonomous driving driver, and I will provide you with the environment information including Ego Car Information, Agents Information and Map Information.</i></p> <p><i>Environment: <map></i></p> <p><i>Routing instructions: Go straight in 9.01 m. Turn right in 119.93 m.</i></p> <p><i>Please predict the future waypoints based on the given environmental information and routing instructions.</i></p> <p><i>Final Answer:</i></p>

Fig. S3: Prompt template for fine-tuning stage.

the next 8 seconds falls below 0.5 meters. An illustration of the input template is provided in Fig. S3.

B Closed-loop Metrics

In this section, we elucidate the metrics of closed-loop evaluation deployed within the nuPlan [4] framework. The calculation for the composite metric *Score* is detailed in Formula 6.

Drivable Area Compliance (Drivable) Ego should remain within the designated drivable area. If a frame is identified where the maximum distance from any corner of the ego’s bounding box to the nearest drivable area exceeds a pre-determined threshold, the drivable area compliance score is assigned a value of 0; otherwise, it is assigned a value of 1.

Driving Direction Compliance (Direct.) The evaluation of the ego’s compliance with the correct driving direction is encapsulated within this metric. It stipulates that a distance traversed in the opposite direction of less than 2 meters within a 1-second interval is deemed compliant, warranting a score of 1. A traversal exceeding 6 meters within the same timeframe indicates a significant deviation from compliance, thus yielding a score of 0. Intermediate distances are assigned a proportional score of 0.5.

Ego is Comfortable (Comf.) This metric quantifies the comfort of the trajectory based on a series of kinematic and dynamic thresholds including longitudinal acceleration, lateral acceleration, yaw acceleration, yaw velocity, longitudinal jerk, and overall jerk magnitude. Compliance across all specified parameters results in a trajectory being classified as "comfortable", meriting a score of 1; otherwise, the score is 0.

Ego Progress Along Expert Route (Prog.) This metric represents the ratio of the ego’s progress per frame to that of an expertly defined route. The closer the ego’s progress is to the expert route’s progress, the higher the score, with the maximum score being 1.

No Ego At-fault Collisions (Coll.) This metric is integral to the safety evaluation, quantifying instances where the ego is directly responsible for collisions. An absence of at-fault collisions throughout the evaluation period scores a 1. A singular collision with a static object, such as a traffic cone, is deemed a minor infraction, scoring a 0.5, whereas all other scenarios result in a score of 0, accentuating the paramount importance of collision avoidance.

Speed Limit Compliance (Lim.) The ego’s adherence to speed regulations is scrutinized by calculating the average instance of speed limit violations per frame. This metric deducts points based on the proximity of the violation to the maximum speed threshold, promoting strict compliance with speed limits.

Time to Collision within Bound (TTC) This metric evaluates the hypothetical time to collision (TTC) with any external agent if the ego were to continue on its trajectory with unaltered speed and heading. A TTC exceeding 0.95 seconds is considered safe, thus earning a score of 1. Lower TTC values signify elevated risk, consequently scoring a 0, highlighting the significance of maintaining a safe buffer from other road users.

Making Progress (MP) An ancillary metric to the Ego Progress Along Expert Route, it assigns a score of 1 if the progress exceeds a threshold of 0.2, otherwise scoring 0. Though not directly incorporated into the main text due to its derivative nature, it contributes to the final score.

Score The final scenario score is calculated by combining the above metrics in a predetermined manner, providing a comprehensive assessment of the autonomous vehicle’s performance within the evaluated scenarios:

$$Score = (Prog * 5 + TTC * 5 + Lim * 4 + Comf * 2) \div 16 \\ *Coll * Drivable * MP * Direct \quad (6)$$

C Scenario Types

In this section, we delineate 14 scenario types employed in both the training and evaluation which is consistent with the nuPlan Challenge 2023 [30]. These scenarios encompass a broad spectrum of driving conditions to evaluate the adaptability and planning capabilities of autonomous vehicles. The scenarios are categorized as follows:

Behind Long Vehicle (type 0): The ego vehicle is positioned behind a long vehicle, maintaining a longitudinal distance of 3 to 10 meters within the same lane, where the lateral distance is less than 0.5 meters.

Changing Lane (type 1): Initiates a maneuver to transition towards an adjacent lane at the beginning of the scenario.

Following Lane with Lead (type 2): Involves the ego vehicle following a leading vehicle that is moving in the same lane with a velocity exceeding 3.5 m/s and a longitudinal distance of less than 7.5 meters.

High Lateral Acceleration (type 3): Characterized by the ego vehicle experiencing high acceleration ($1.5 < \text{acceleration} < 3 \text{ m/s}^2$) across the lateral axis, accompanied by a high yaw rate, without executing a turn.

High Magnitude Speed (type 4): The ego vehicle achieves a high velocity magnitude exceeding 9 m/s with low acceleration.

Low Magnitude Speed (type 5): Ego vehicle moves at low velocity magnitude ($0.3 < \text{velocity} < 1.2 \text{ m/s}$) with low acceleration, without coming to a stop.

Near Multiple Vehicles (type 6): The ego vehicle is proximate to multiple (more than six) moving vehicles within a distance of less than 8 meters while maintaining a velocity of more than 6 m/s.

Starting Left Turn (type 7): Marks the commencement of a left turn by the ego vehicle across an intersection area, without being halted.

Starting Right Turn (type 8): Marks the commencement of a right turn by the ego vehicle across an intersection area, without being halted.

Starting Straight Traffic Light Intersection Traversal (type 9): The ego vehicle begins to traverse straight through an intersection controlled by traffic lights, without being stopped.

Stationary in Traffic (type 10): The ego vehicle remains stationary amidst traffic, surrounded by multiple (more than six) vehicles within an 8-meter radius.

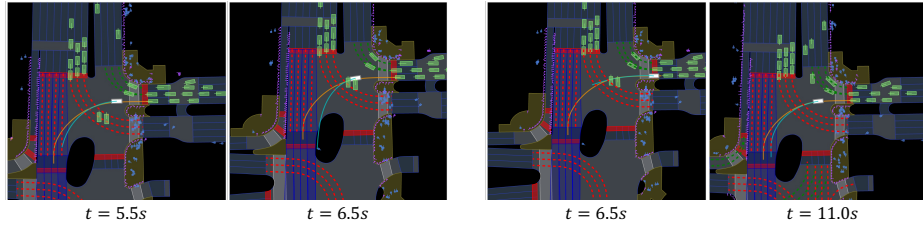
Stopping with Lead (type 11): The scenario begins with the ego vehicle initiating deceleration (acceleration magnitude less than -0.6 m/s^2 , velocity magnitude less than 0.3 m/s) due to the presence of a leading vehicle ahead within a distance of less than 6 meters.

Traversing Pickup/Dropoff (type 12): The ego vehicle navigates through a pickup or drop-off area without stopping.

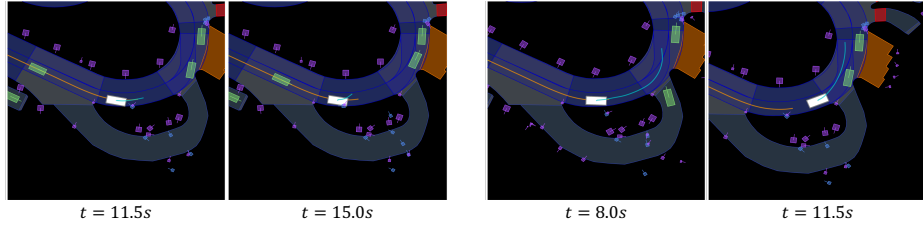
Waiting for Pedestrian to Cross (type 13): The ego vehicle waits for a pedestrian, who is within an 8-meter distance and less than 1.5 seconds away from the intersection, to cross a crosswalk. This occurs while the ego vehicle is not stopped and the pedestrian is not located in a pickup or drop-off area.

D Visualization

Fig. S4 additionally showcases a series of our visualization results and demonstrates its superior performance to GameFormer [18] across multiple metrics.



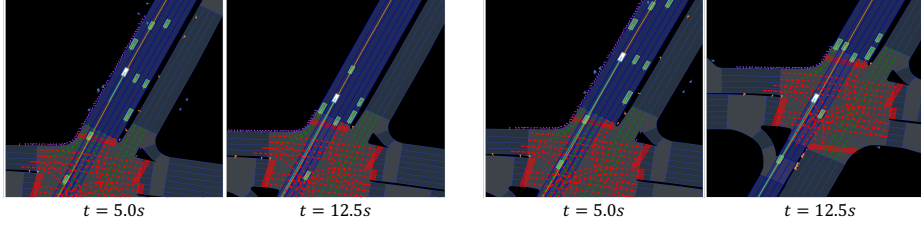
(a) GameFormer collides with other vehicles at 6.5s; AsyncDriver first yield to the vehicle going straight, then passes smoothly.



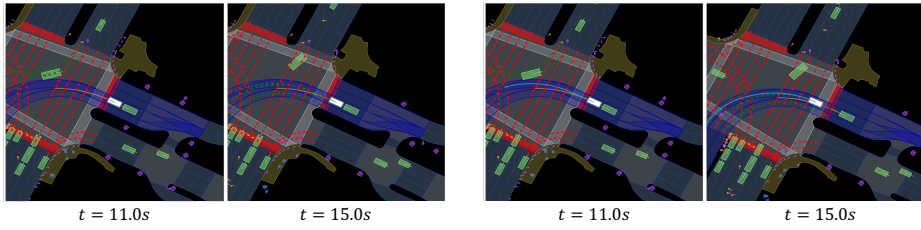
(b) GameFormer, upon reaching 11.5s, finds it difficult to evade pedestrians ahead, resulting in a collision at 15.0s; AsyncDriver, anticipating the situation in advance, passes smoothly before the pedestrians approach.

References

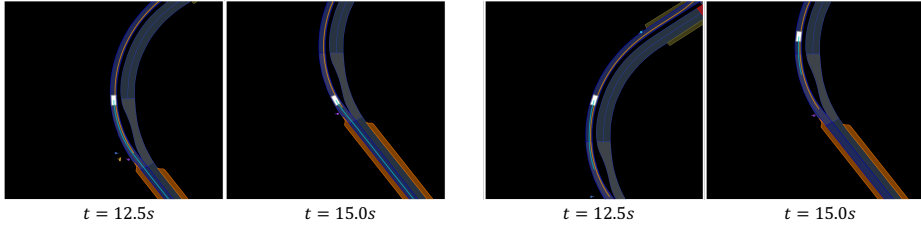
1. Achiam, J., Adler, S., Agarwal, S., Ahmad, L., Akkaya, I., Aleman, F.L., Almeida, D., Altenschmidt, J., Altman, S., Anadkat, S., et al.: Gpt-4 technical report. arXiv preprint arXiv:2303.08774 (2023)
2. Bacha, A., Bauman, C., Faruque, R., Fleming, M., Terwelp, C., Reinholtz, C., Hong, D., Wicks, A., Alberi, T., Anderson, D., et al.: Odin: Team victortango’s entry in the darpa urban challenge. *Journal of field Robotics* **25**(8), 467–492 (2008)
3. Baidu: Apollo auto. <https://github.com/ApolloAuto/apollo> (July 2019)
4. Caesar, H., Kabzan, J., Tan, K.S., Fong, W.K., Wolff, E., Lang, A., Fletcher, L., Beijbom, O., Omari, S.: nuplan: A closed-loop ml-based planning benchmark for autonomous vehicles. arXiv preprint arXiv:2106.11810 (2021)
5. Chen, L., Zhang, Y., Ren, S., Zhao, H., Cai, Z., Wang, Y., Wang, P., Liu, T., Chang, B.: Towards end-to-end embodied decision making via multi-modal large language model: Explorations with gpt4-vision and beyond. arXiv preprint arXiv:2310.02071 (2023)
6. Chen, L., Li, Y., Huang, C., Li, B., Xing, Y., Tian, D., Li, L., Hu, Z., Na, X., Li, Z., et al.: Milestones in autonomous driving and intelligent vehicles: Survey of surveys. *IEEE Transactions on Intelligent Vehicles* **8**(2), 1046–1056 (2022)
7. Chen, L., Sinavski, O., Hünermann, J., Karnsund, A., Willmott, A.J., Birch, D., Maund, D., Shotton, J.: Driving with llms: Fusing object-level vector modality for explainable autonomous driving. arXiv preprint arXiv:2310.01957 (2023)
8. Cui, C., Ma, Y., Cao, X., Ye, W., Wang, Z.: Receive, reason, and react: Drive as you say with large language models in autonomous vehicles. arXiv preprint arXiv:2310.08034 (2023)
9. Cui, C., Ma, Y., Cao, X., Ye, W., Zhou, Y., Liang, K., Chen, J., Lu, J., Yang, Z., Liao, K.D., et al.: A survey on multimodal large language models for autonomous driving. In: *Proceedings of the IEEE/CVF Winter Conference on Applications of Computer Vision*. pp. 958–979 (2024)



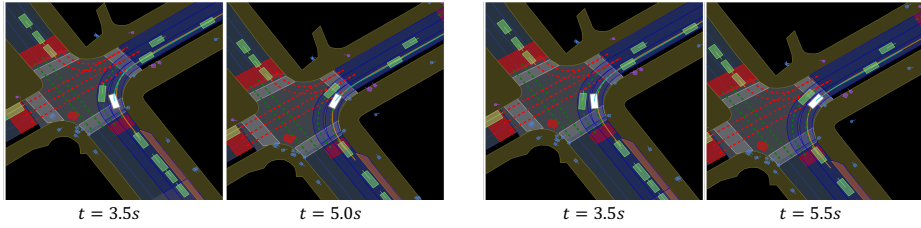
(c) GameFormer makes a misjudgment about the traffic light status at 5.0s, noticeably decelerating, leading to its failure to enter the intersection at 12.5s due to slow progress; AsyncDriver maintains a steady speed and enters the intersection smoothly.



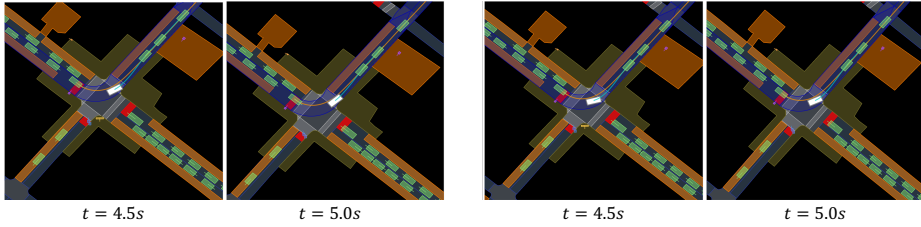
(d) GameFormer, after the traffic light turns from red to green at 11.0s, fails to start promptly and remains stationary at 15.0s; AsyncDriver starts on time and enters the intersection.



(e) At 12.5 seconds, when a pedestrian appears ahead, GameFormer does not evade or decelerate; AsyncDriver clearly brakes.



(f) GameFormer gets too close to the adjacent car while turning, increasing the risk of collision; AsyncDriver travels almost parallel to the neighboring car, greatly enhancing safety.



(g) GameFormer turns out of the drivable area; AsyncDriver does not.

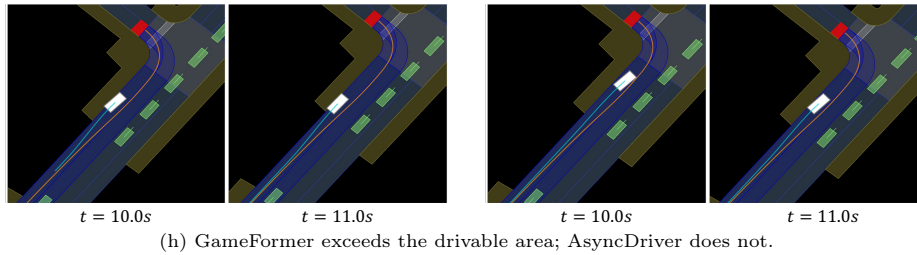


Fig. S4: The visualization results of GameFormer and AsyncDriver in various scenarios, with corresponding analytical explanations provided in subcaptions. The left two columns display the results for GameFormer, while the right two columns show the results for AsyncDriver.

10. Dauner, D., Hallgarten, M., Geiger, A., Chitta, K.: Parting with misconceptions about learning-based vehicle motion planning. arXiv preprint arXiv:2306.07962 (2023)
11. Fan, H., Zhu, F., Liu, C., Zhang, L., Zhuang, L., Li, D., Zhu, W., Hu, J., Li, H., Kong, Q.: Baidu apollo em motion planner. arXiv preprint arXiv:1807.08048 (2018)
12. Fu, D., Li, X., Wen, L., Dou, M., Cai, P., Shi, B., Qiao, Y.: Drive like a human: Rethinking autonomous driving with large language models. In: Proceedings of the IEEE/CVF Winter Conference on Applications of Computer Vision. pp. 910–919 (2024)
13. Hallgarten, M., Stoll, M., Zell, A.: From prediction to planning with goal conditioned lane graph traversals. arXiv preprint arXiv:2302.07753 (2023)
14. Han, W., Guo, D., Xu, C.Z., Shen, J.: Dme-driver: Integrating human decision logic and 3d scene perception in autonomous driving. arXiv preprint arXiv:2401.03641 (2024)
15. Hu, E.J., Shen, Y., Wallis, P., Allen-Zhu, Z., Li, Y., Wang, S., Wang, L., Chen, W.: Lora: Low-rank adaptation of large language models. arXiv preprint arXiv:2106.09685 (2021)
16. Hu, S., Chen, L., Wu, P., Li, H., Yan, J., Tao, D.: St-p3: End-to-end vision-based autonomous driving via spatial-temporal feature learning. In: European Conference on Computer Vision. pp. 533–549. Springer (2022)
17. Hu, Y., Yang, J., Chen, L., Li, K., Sima, C., Zhu, X., Chai, S., Du, S., Lin, T., Wang, W., et al.: Planning-oriented autonomous driving. In: Proceedings of the IEEE/CVF Conference on Computer Vision and Pattern Recognition. pp. 17853–17862 (2023)
18. Huang, Z., Liu, H., Lv, C.: Gameformer: Game-theoretic modeling and learning of transformer-based interactive prediction and planning for autonomous driving. arXiv preprint arXiv:2303.05760 (2023)
19. Jin, Y., Shen, X., Peng, H., Liu, X., Qin, J., Li, J., Xie, J., Gao, P., Zhou, G., Gong, J.: Surrealdriver: Designing generative driver agent simulation framework in urban contexts based on large language model. arXiv preprint arXiv:2309.13193 (2023)
20. Kendall, A., Hawke, J., Janz, D., Mazur, P., Reda, D., Allen, J.M., Lam, V.D., Bewley, A., Shah, A.: Learning to drive in a day. In: 2019 International Conference on Robotics and Automation (ICRA). pp. 8248–8254. IEEE (2019)
21. Kesting, A., Treiber, M., Helbing, D.: General lane-changing model mobil for car-following models. Transportation Research Record: Journal of the Transportation

- Research Board p. 86–94 (Jan 2007). <https://doi.org/10.3141/1999-10>, <http://dx.doi.org/10.3141/1999-10>
22. Keysan, A., Look, A., Kosman, E., Gürsun, G., Wagner, J., Yu, Y., Rakitsch, B.: Can you text what is happening? integrating pre-trained language encoders into trajectory prediction models for autonomous driving. arXiv preprint arXiv:2309.05282 (2023)
 23. Leonard, J., How, J., Teller, S., Berger, M., Campbell, S., Fiore, G., Fletcher, L., Frazzoli, E., Huang, A., Karaman, S., et al.: A perception-driven autonomous urban vehicle. *Journal of Field Robotics* **25**(10), 727–774 (2008)
 24. Li, Z., Nie, F., Sun, Q., Da, F., Zhao, H.: Boosting offline reinforcement learning for autonomous driving with hierarchical latent skills. arXiv preprint arXiv:2309.13614 (2023)
 25. Liu, J., Hang, P., Qi, X., Wang, J., Sun, J.: Mtd-gpt: A multi-task decision-making gpt model for autonomous driving at unsignalized intersections. In: 2023 IEEE 26th International Conference on Intelligent Transportation Systems (ITSC). pp. 5154–5161. IEEE (2023)
 26. Ma, Y., Cao, Y., Sun, J., Pavone, M., Xiao, C.: Dolphins: Multimodal language model for driving. arXiv preprint arXiv:2312.00438 (2023)
 27. Ma, Y., Cui, C., Cao, X., Ye, W., Liu, P., Lu, J., Abdelraouf, A., Gupta, R., Han, K., Bera, A., et al.: Lampilot: An open benchmark dataset for autonomous driving with language model programs. arXiv preprint arXiv:2312.04372 (2023)
 28. Mao, J., Qian, Y., Zhao, H., Wang, Y.: Gpt-driver: Learning to drive with gpt. arXiv preprint arXiv:2310.01415 (2023)
 29. Mao, J., Ye, J., Qian, Y., Pavone, M., Wang, Y.: A language agent for autonomous driving. arXiv preprint arXiv:2311.10813 (2023)
 30. Motional: nuplan challenge. <https://github.com/motional/nuplan-devkit> (2023)
 31. Nie, M., Peng, R., Wang, C., Cai, X., Han, J., Xu, H., Zhang, L.: Reason2drive: Towards interpretable and chain-based reasoning for autonomous driving. arXiv preprint arXiv:2312.03661 (2023)
 32. Renz, K., Chitta, K., Mercea, O.B., Koepke, A., Akata, Z., Geiger, A.: Plant: Explainable planning transformers via object-level representations. arXiv preprint arXiv:2210.14222 (2022)
 33. Scheel, O., Bergamini, L., Wolczyk, M., Osiński, B., Ondruska, P.: Urban driver: Learning to drive from real-world demonstrations using policy gradients. In: Conference on Robot Learning. pp. 718–728. PMLR (2022)
 34. Sha, H., Mu, Y., Jiang, Y., Chen, L., Xu, C., Luo, P., Li, S.E., Tomizuka, M., Zhan, W., Ding, M.: Languagempc: Large language models as decision makers for autonomous driving. arXiv preprint arXiv:2310.03026 (2023)
 35. Shao, H., Hu, Y., Wang, L., Waslander, S.L., Liu, Y., Li, H.: Lmdrive: Closed-loop end-to-end driving with large language models. arXiv preprint arXiv:2312.07488 (2023)
 36. Sharan, S., Pittaluga, F., Chandraker, M., et al.: Llm-assist: Enhancing closed-loop planning with language-based reasoning. arXiv preprint arXiv:2401.00125 (2023)
 37. Sima, C., Renz, K., Chitta, K., Chen, L., Zhang, H., Xie, C., Luo, P., Geiger, A., Li, H.: Drivelm: Driving with graph visual question answering. arXiv preprint arXiv:2312.14150 (2023)
 38. Touvron, H., Martin, L., Stone, K., Albert, P., Almahairi, A., Babaei, Y., Bashlykov, N., Batra, S., Bhargava, P., Bhosale, S., et al.: Llama 2: Open foundation and fine-tuned chat models. arXiv preprint arXiv:2307.09288 (2023)

39. Treiber, M., Hennecke, A., Helbing, D.: Congested traffic states in empirical observations and microscopic simulations. *Physical Review E* p. 1805–1824 (Jul 2002). <https://doi.org/10.1103/physreve.62.1805>, <http://dx.doi.org/10.1103/physreve.62.1805>
40. Urmsion, C., Anhalt, J., Bagnell, D., Baker, C., Bittner, R., Clark, M., Dolan, J., Duggins, D., Galatali, T., Geyer, C., et al.: Autonomous driving in urban environments: Boss and the urban challenge. *Journal of field Robotics* **25**(8), 425–466 (2008)
41. Wang, S., Zhu, Y., Li, Z., Wang, Y., Li, L., He, Z.: Chatgpt as your vehicle co-pilot: An initial attempt. *IEEE Transactions on Intelligent Vehicles* (2023)
42. Wang, W., Xie, J., Hu, C., Zou, H., Fan, J., Tong, W., Wen, Y., Wu, S., Deng, H., Li, Z., et al.: Drivemlm: Aligning multi-modal large language models with behavioral planning states for autonomous driving. arXiv preprint arXiv:2312.09245 (2023)
43. Wang, Y., Jiao, R., Lang, C., Zhan, S.S., Huang, C., Wang, Z., Yang, Z., Zhu, Q.: Empowering autonomous driving with large language models: A safety perspective. arXiv preprint arXiv:2312.00812 (2023)
44. Wen, L., Fu, D., Li, X., Cai, X., Ma, T., Cai, P., Dou, M., Shi, B., He, L., Qiao, Y.: Dilu: A knowledge-driven approach to autonomous driving with large language models. arXiv preprint arXiv:2309.16292 (2023)
45. Xu, Z., Zhang, Y., Xie, E., Zhao, Z., Guo, Y., Wong, K.K., Li, Z., Zhao, H.: Drivegpt4: Interpretable end-to-end autonomous driving via large language model. arXiv preprint arXiv:2310.01412 (2023)
46. Yang, Z., Jia, X., Li, H., Yan, J.: A survey of large language models for autonomous driving. arXiv preprint arXiv:2311.01043 (2023)
47. Yuan, J., Sun, S., Omeiza, D., Zhao, B., Newman, P., Kunze, L., Gadd, M.: Rag-driver: Generalisable driving explanations with retrieval-augmented in-context learning in multi-modal large language model. arXiv preprint arXiv:2402.10828 (2024)
48. Zhou, X., Liu, M., Zagar, B.L., Yurtsever, E., Knoll, A.C.: Vision language models in autonomous driving and intelligent transportation systems. arXiv preprint arXiv:2310.14414 (2023)